MQES
Macroscopic quantum experiments in space using massive mechanical resonators
(Po P5401000400)

	Name/Title	Signature	Date
Prepared by:	Rainer Kaltenbaek University of Vienna		04.02.2013
Study authors:	Rainer Kaltenbaek[1], Gerald Hechenblaikner[2], Nikolai Kiesel[1], Florian Blaser[1], Simon Gröblacher[3,1], Sebastian Hofer[4,1], Michael R. Vanner[1], Witlef Wieczorek[1], Keith C. Schwab[3], Ulrich Johann[2], and Markus Aspelmeyer[1]		
Affiliations:	[1] Vienna Center for Quantum Science and Technology, Faculty of Physics, University of Vienna [2] EADS Astrium Friedrichshafen, Immenstaad [3] Applied Physics, California Institute of Technology, Pasadena [4] Institut für Theoretische Physik, Leibniz Universität, Hannover		
Technical management:	Eric Wille TEC-MMO		
Vienna Center for Quantum Science and Technology Faculty of Physics, University of Vienna Boltzmanngasse 5, 1090 Vienna, Austria			

Page intentionally left blank

ESA STUDY FINAL REPORT		
ESA Contract No: Po P5401000400	SUBJECT: Macroscopic quantum experiments in space using massive mechanical resonators	CONTRACTOR: UNIV WIEN EXPERIMENTALPHYSIK BOLTZMANNGASSE 5 1090 WIEN
ESA CR()No:	No. of Volumes:.... This is Volume No:....	CONTRACTOR'S REFERENCE:

ABSTRACT

One of the central challenges in fundamental physics is to understand the laws of physics in parameter regimes that are hitherto untested, and where we may expect deviations from standard quantum and gravitational physics. Such deviations, but also confirmations of the validity of standard physics over a larger range of parameters, may guide us in the formulation of new theoretical models, like a unified theory of quantum physics and gravity. Several space missions have been planned to investigate possible deviations from general relativity (e.g., STE-Quest and Microscope). But new physics should also lead to deviations from quantum theory if one performs quantum experiments with objects that are massive enough that their gravity may start to play a role. In particular, quantum physics allows for the possibility of a massive object to be in a superposition of being in two distinct places at the same time. Will that result in a corresponding superposition of different spacetimes? Is quantum physics still valid in a regime where such questions become relevant? The rapid progress in the new field of quantum optomechanics promises that we will soon be able to perform experiments with macroscopic objects that will vastly expand the parameter regime over which one can test quantum physics, possibly allowing for experimentally addressing the questions stated above. In the present study, we propose two such quantum optomechanical experiments (WAX and DECIDE). Both of these experiments require a space environment and aim at testing the predictions of quantum theory in a completely new parameter regime and comparing the predictions of quantum physics with the predictions of "macrorealistic" modifications of quantum theory. These modifications predict a transition from quantum to classical behavior for increasingly massive systems. We picked DECIDE for a closer investigation and for the definition of a detailed preliminary design.

The work described in this report was done under ESA Contract. Responsibility for the contents resides in the author or organisation that prepared it.

Names of authors: Rainer Kaltenbaek

NAME OF ESA STUDY MANAGER: Eric Wille, TEC-MMO DIV: DIRECTORATE:	ESA BUDGET HEADING:

Page intentionally left blank

Table of Contents

1 List of Abbreviations 7

2 Introduction and Motivation 9
2.1 Quantum superpositions and interference . . . 9
2.2 Quantum effects and macroscopic objects . . . 10
2.3 Quantum optomechanics . . . 10
2.4 Motivation for quantum experiments with macroscopic objects . . . 11
2.5 Quantum decoherence and macrorealism . . . 11
2.5.1 Quantum decoherence . . . 11
2.5.2 Macrorealism . . . 12

3 Proposed optomechanical experiments for a space environment 13
3.1 Wave-function expansion of massive objects (WAX) . . . 14
3.2 Decoherence in a double-slit experiment (DECIDE) . . . 16
3.3 Baseline-parameters and scientific requirements . . . 19
3.4 Technical Requirements . . . 19
3.5 Trade-off and conceptual design selection . . . 20

4 Preliminary design for DECIDE 23
4.1 The thermal-shield assembly . . . 23
4.2 The optical-bench assembly . . . 23
4.3 The laser assembly and the detection assembly . . . 24
4.4 The data-preanalysis assembly . . . 26

5 Conclusions 27
5.1 Issues that need more detailed analysis or further study . . . 27
5.1.1 COM heating due to intracavity power fluctuations . . . 27
5.1.2 Cooling the radial degree of freedom . . . 27
5.1.3 Loading nanospheres into the optical trap . . . 28
5.1.4 Manipulation of the nanospheres . . . 28
5.2 Critical issues and possible solutions . . . 28
5.2.1 Preparing the quantum superposition with short-wavelength UV light . . . 28
5.2.2 Possible alternatives to the use of short-wavelength UV light . . . 29
5.3 Technology roadmap . . . 30

Bibliography 31

Page intentionally left blank

1 List of Abbreviations

AOM	**a**cousto-**o**ptic **m**odulator
BS	**b**eam **s**plitter
CCD	**c**harge-**c**oupled **d**evice
CMOS	**c**omplementary **m**etal **o**xide **s**emiconductor
COM	**c**enter **of** **m**ass
CSL	**c**ontinuous **s**pontaneous **l**ocalization
DECIDE	**Dec**oherence **i**n a **d**ouble-slit **e**xperiment
DP model	the macrorealistic model of **D**iósi and **P**enrose
EOM	**e**lectro-**o**ptic **m**odulator
FG	**f**unction **g**enerator
FSR	**f**ree **s**pectral **r**ange
FT	**f**eed **t**hrough
GRW	**G**hirardi-**R**imini-**W**eber
IR	**i**nfra **r**ed
K model	the macrorealistic model of **K**árolzházy
LISA	**L**aser **i**nterferometer **s**pace **a**ntenna
LM	**l**oading **m**echanism
MAQRO	**Ma**croscopic **q**uantum **r**es**o**nators
MR	**m**acro**r**ealism
PBS	**p**olarizing **b**eam **s**plitter
PDH	**P**ound **D**rever **H**all
PM	**p**olarization **m**aintaining
QG model	the "**q**uantum **g**ravity"-based model of Ellis and co-workers
QM	**q**uantum **m**echanics
RIN	**r**elative **i**ntensity **n**oise
STA	**s**tate of **t**he **a**rt
TBD	**t**o **b**e **d**etermined
UV	**u**tra **v**iolet
WAX	**Wa**ve-packet e**x**pansion of massive objects

Page intentionally left blank

2 Introduction and Motivation

Here, we will provide a quick review of the principles behind matter-wave interference. We will consider the question under which conditions such effects can also be observed for macroscopic systems and whether there will occur a transition from quantum to classical behavior as the system size and/or mass increases.

2.1 Quantum superpositions and interference

The concepts of quantum physics often challenge our understanding. They not only seem far removed from our everyday experience but at times are in direct contradiction to it. One of the most illustrative examples is quantum superposition where a system can simultaneously be in clearly distinct states. This concept lies at the heart of quantum physics. A famous example is the double-slit experiment (see, e. g., Ref. [33]): consider a source (S) of physical systems like, e.g., photons or atoms. At some distance there is a flat detection screen (D) that can detect the position where entities emitted by S hit the screen D. A wall (W) is put between S and D, and that wall has two narrow but long, parallel slits.

If the source, S, emits waves, e.g., water waves, they can pass through both slits at the same time. Behind W, the waves emitted from the two slits can then coherently add up and form an interference pattern, i.e., in some places the waves will cancel (destructive interference), while they will add up at other spots (constructive interference). The same is true for electromagnetic waves in classical electrodynamics.

Should S emit particles instead of waves, it is tempting to assume that each particle like, e.g., an atom can only reach D and be detected if, and only if, the particle passes through one or the other slit in W. Under this assumption, the detection probability at D will just be an incoherent sum of the probabilities of particles going either through one slit or the other. However, quantum physics predicts that, under certain conditions, particles can show interference, too. The concept behind this effect is the quantum superposition of two probability amplitudes ψ_1 and ψ_2 for the particle passing through the first or the second slit, respectively. If it is **in principle** impossible to know which slit the particle went through, then the probability amplitude for detecting the particle at a specific point on screen D is the coherent sum of the two individual amplitudes, i.e., $\psi_1 + \psi_2$.

The probability for detecting the particle then is the modulus square of that sum, i.e., $|\psi_1 + \psi_2|^2$. On the other hand, if there exists information about the path of the, then the probability for detecting the particle is $|\psi_1|^2 + |\psi_2|^2$. In the first case, we see interference, in the second case, we do not. That means, that we will observe quantum superposition and interference between different possibilities if and only if there is no way to tell which of the two possibilities was actually realized.

2.2 Quantum effects and macroscopic objects

The question is why we do not observe such interference effects for macroscopic objects. If we believe quantum physics to describe our world well, then the same laws of physics that lead to the interference of an atom or a molecule with itself also apply to macroscopic objects.

Schrödinger investigated this question in a famous gedankenexperiment, which is known as **Schrödinger's cat**: if one believes that quantum physics is valid even for macroscopic systems, then it should be possible to prepare a cat in a quantum superposition of clearly distinct states like dead and alive [73]. The essential feature of this gedankenexperiment is that the cat as well as the "diabolic mechanism" [73] that releases a poison and can kill the cat are all contained within a box that prevents the outside world from knowing the state of the cat. That means, outside the box, it is impossible to know what happens to the cat and, therefore, quantum physics will predict that such a superposition of a cat being dead and alive is possible.

However, to isolate a system well enough from the environment to allow for such superpositions, becomes increasingly difficult for large systems. Since the early days of quantum theory, scientists have tried to observe quantum superposition and quantum interference or wave-like behavior for increasingly massive systems, e.g., for electrons [16, 75], atoms and molecules [30], as well as for neutrons [77]. Over the last decade or so, the group of M. Arndt has observed matter-wave interference for increasingly massive molecules (see, e.g., Refs. [4, 14, 35, 43, 46] consisting of many hundreds or even thousands of atoms. While these experiments follow a bottom-up approach of showing matter-wave interference with increasingly massive and complex objects, the novel field of quantum optomechanics follows a complementary, bottom-down approach where the goal is to bring massive classical systems down into the quantum regime. Both of these approaches have the same **central question**: is there a limit to the size/mass/complexity of objects to still exhibit wave-like behavior like interference?

2.3 Quantum optomechanics

Optomechanics is the field investigating the interaction between light and mechanical properties of a system like, e.g., the center-of-mass (COM) motion of a mechanical oscillator. Quantum optomechanics investigates the same topic but under conditions where the quantization of the electromagnetic field as well as the quantization of mechanical degrees of freedom becomes relevant.

The action of radiation pressure on matter has already been suggested by Kepler in the 17$^{\text{th}}$ century [49, 50]. He suspected that the light emitted by the sun affects the inclination of the tails of comets. Related predictions about the strength of this radiation-pressure force were later made by Maxwell [58] and Bartoli [9] and were first confirmed in experiments by Lebedev [52] and Nichols and Hull [60].

In the 1960s and 70s, Braginsky and others studied the influence of radiation pressure in the context of gravitational wave antennae, in particular, how the quantum nature of light affects the sensitivity of interferometers [11, 13, 17, 59]. First experiments on radiation-pressure effects in cavities [12] with macroscopic mechanical oscillators were performed in the 1980s [25].

Subsequently, several theoretical proposals for quantum optics experiments in a cavity using radiation-pressure effects were published, such as the generation of squeezed light [32, 55], quantum non-demolition measurements of photon numbers [44, 65], feedback-cooling of the mechanical motion [56] (see also Ref. [20]), entanglement between the optical and the mechanical mode [10, 54, 57], and the quantum-state transfer from the light field to the mechanical oscillator [78]. However, first experiments were only realized in recent years (except for Ref. [25]): measurements of the motion of a mechanical oscillator [3, 15, 76], parametric amplification of the mechanical motion [51], cavity cooling of the mechanical resonator [2, 22, 38, 72], cryogenic cavity cooling [40, 42, 62, 71] and strongly coupled optomechanics [41].

Recently, several research groups have achieved the cooling of the COM motion of mechanical oscillators close to the ground-state of motion [18, 61, 74]. This has been a long-standing goal for quantum optomechanics and is the first step towards preparing the mechanical system in interesting states like quantum superposition states, either for quantum information processing [7, 61] or for fundamental tests of quantum physics as we have discussed above.

2.4 Motivation for quantum experiments with macroscopic objects

The questions we would like to address with this macroscopic quantum superpositions are:

- will gravitation lead to modifications of quantum physics for very massive objects?
- are macroscopic quantum superpositions at all possible or are there yet unknown decoherence mechanisms?
- the short de-Broglie wavelength of massive particles can be used for high sensitivity matter-wave interferometry, possibly allowing for more accurate tests of general relativity (equivalence principle, Lens-Thirring, gravitational wave detection, ...) or for more precise measurements of gravitational fields, e.g., in Earth observation

2.5 Quantum decoherence and macrorealism

2.5.1 Quantum decoherence

In practical implementations, quantum systems can never be fully isolated from their environment. Such imperfect isolation results in an apparent loss of coherence for quantum superpositions. This loss of coherence due to interaction with the environment is called quantum decoherence.

Typical sources of quantum decoherence are:

- collisions with gas molecules
- scattering/emission/absorption of blackbody radiation
- coupling to the environment via a mechanical suspension

Additional effects detrimental for matter-wave interference with massive particles will be taken into account via the technical requirements of the experiment. These are, e.g., micro-thruster force noise, charging due to cosmic radiation, and gravitational rest gradients.

In the presence of weak quantum decoherence (long-wavelength limit), the time evolution of the density matrix $\hat{\rho}$ of a quantum system can be described via the following equation [34, 36, 45]:

$$\frac{\partial}{\partial t}\hat{\rho}(t) = -\frac{\mathrm{i}}{\hbar}\left[\hat{H}, \hat{\rho}(t)\right] - \Lambda\left[\hat{x}, \left[\hat{x}, \hat{\rho}(t)\right]\right]. \tag{2.1}$$

where $h = 2\pi\hbar$ is Planck's constant, $\hat{x}$ is the position operator, $\hat{H}$ is the Hamiltonian, and Λ describes the strength of the interaction between our quantum system and its environment. For an ideally isolated quantum system, i.e., if there is no decoherence at all, we have $\Lambda = 0$. That means, if there is no interaction with the environment, we can make arbitrarily large superpositions like, e.g., Schrödinger's cat.

2.5.2 Macrorealism

There are, however, models that suggest a modification of quantum theory such $\Lambda \neq 0$ even for completely isolated systems due to additional decoherence mechanisms that typically depend on the mass and/or the size of the quantum system. This way, increasingly large/massive systems will behave more and more classical. Macroscopic superpositions like that of Schrödinger's cat would then be impossible to observe because they decohere nearly immediately. Such models are called collapse models or macrorealistic models.

These additional decoherence mechanisms can also be described via a decoherence parameter Λ_{MR} [34, 47, 68, 70]. The decoherence predicted by macrorealistic models is an additional effect and results in an effective decoherence parameter $\Lambda = \Lambda_{\mathrm{QM}} + \Lambda_{\mathrm{MR}}$, where Λ_{QM} is the decoherence parameter describing the overall effects of standard quantum decoherence.

In the following, we will provide a short outline of several of such models:

- **the continuous-spontaneous-localization (CSL) model:**
  a heuristic model predicting a continuous transition between the quantum and the classical regime. It is based upon the work of Ghirardi, Rimini and Weber (GRW) [36] and Pearle [63]. See also Refs. [21, 39].
- **the quantum-gravity (QG) model:**
  A model suggested by Ellis, Mavromatos, Nanopoulos, and Mohanty [27–29]. It suggests a modification of quantum theory and decoherence of macroscopic superpositions due to quantum gravity.
- **the model of Diósi and Penrose (DP):**
  Diósi (see, e.g., Refs. [23, 24]) and Penrose (see, e.g., Ref. [64]) suggested models where gravity leads to the collapse of macroscopic superpositions. The two models are based on fundamentally different approaches, but make essentially identical predictions. We denote this as the DP model.
- **the model of Károlyházy (K model):**
  The model of Károlyázy [48] predicts decoherence due to quantum fluctuations of the spacetime metric.

We will denote the decoherence parameters corresponding to these different models as Λ_{CSL}, Λ_{QG}, Λ_{DP}, and Λ_{K}, respectively.

3 Proposed optomechanical experiments for a space environment

As we have mentioned in subsection 2.5.1, one of the most prominent decoherence mechanisms in optomechanical systems is the scattering, emission and absorption of phonons via the mechanical suspension of an optomechanical system. Recently, there have been several proposals how to eliminate this decoherence mechanism by using optically trapped nano- or microspheres [8, 19, 67, 69]. In this case, the COM motion of the optically trapped sphere acts is described as a mechanical oscillator, and it can be cooled either via feedback or via side-band cooling. Based on these proposals, several works suggest testing the foundations of quantum physics using such optically trapped systems [47, 68, 70]. The concept of the optical trapping of particles is based on the works of Ashkin (see, e.g., [5, 6]).

Because such systems are not bound to a fixed structure via a mechanical suspension, they are natural candidates for possible future optomechanical experiments in a micro-gravity environment as achievable in space [47]. The most apparent advantages of performing such experiments in a micro-gravity environment are:

- in principle, arbitrarily massive objects can be optically trapped
- for a given mass, the optical power necessary to trap an object is less than in the presence of a strong gravitational field. As a result, the heating due to the trap beam is less, leading to reduced decoherence due to the emission of blackbody radiation
- the power of the trapping beam can be very low - it only has to overcome the thermal energy of the trapped object. This allows for the preparation of nearly arbitrarily large quantum superpositions, i.e., superpositions of a particle being in two very distant positions at the same time.
- at any time, the trapping beam can be switched off in order to observe the free evolution of the quantum state. As we will see below, one can, for example, observe the expansion of the wavefunction of the object once it is released from the trap. A micro-gravity environment allows for the observation of this expansion over long times.

An implicit advantage of using optically trapped particles is the possibility of nearly arbitrarily varying the potential and the frequency of the mechanical oscillator by changing the power of the trapping beam.

As in quantum optomechanics, in general, a prerequisite for performing quantum experiments with optically trapped nanospheres is to prepare their COM motion in a low-entropy state. Very recently, there has been significant progress towards that goal by feedback cooling of the COM motion of nano- and microparticles [37, 53]. The optomechanical experiments we will suggest in the following are all based on the optical trapping of nanospheres inside an optical cavity.

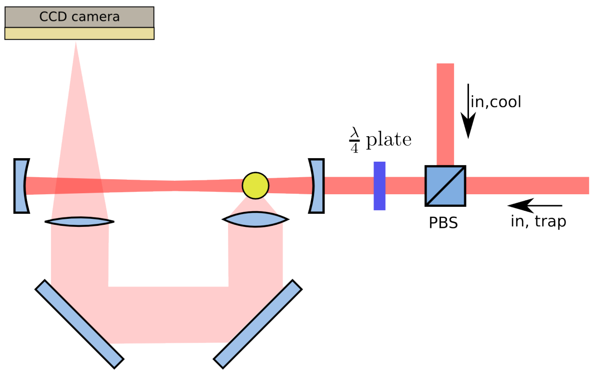

Figure 3.1: **Conceptual design of WAX.** Two infrared beams are overlapped at a polarizing beam splitter and fed into a cavity. The stronger of the two beams is used to trap a nanosphere, the second beam is used to side-band cool the center-of-mass motion of the nanosphere. A combination of two lenses and mirrors is used to image the trapping region onto a CCD or CMOS chip in order to measure the position of the nanosphere. The light-red beam path illustrates the imaging of scattered light onto the camera.

3.1 Wave-function expansion of massive objects (WAX)

The objective of this experiment is to measure the expansion of the wave packet of a massive object as a function of time, and to study possible deviations from the predictions of quantum mechanics due to the influence of macrorealistic decoherence mechanisms (see subsection 2.5.2).

Figure 3.1 shows the conceptual layout of WAX. A typical experimental run of WAX consists of the following steps:

1. load a nanoparticle into an optical trap inside an optical cavity
2. move the particle to a predefined position along the cavity axis
3. cool the COM motion of the nanoparticle close to the quantum ground state
4. switch off the trap and let the particle's wavefunction expand freely for a time t
5. measure the position of the nanoparticle along the cavity axis
6. trap the particle again and repeat the steps above starting from step (2)

After repeating this procedure often enough to get enough data for statistical significance, the width of the distribution of particle positions is determined. This procedure can be performed for various values of t in order to determine the time-dependence of the expansion of the wavefunction. The experimentally determined values can then be compared with the values predicted by quantum theory and with the values predicted by various macrorealistic models.

In general, if the decoherence of a quantum system is described by a decoherence parameter Λ, the square of the width of the expanding wavefunction after a time t is given by:

$$\langle \hat{x}^2(t) \rangle = \langle \hat{x}^2(t) \rangle_s + \frac{2\Lambda\hbar^2}{3m^2} t^3, \tag{3.1}$$

where m is the mass of the nanoparticle, and $\langle \hat{x}^2(t) \rangle_s$ is the square of the width of the wavepacket in the absence of any decoherence. If the system is originally in a thermal state with a mean occupation number n, and if we assume that the state does not change during its release from the optical trap, then the above expression for the square of the width of the wavepacket becomes:

$$\langle \hat{x}^2(t) \rangle = \frac{(1+2n)\hbar}{2m\omega} + \frac{(1+2n)\hbar\omega}{2}\frac{t^2}{m} + \frac{2\Lambda\hbar^2}{3m^2}t^3, \tag{3.2}$$

where ω is the mechanical frequency of the trapped nanosphere.

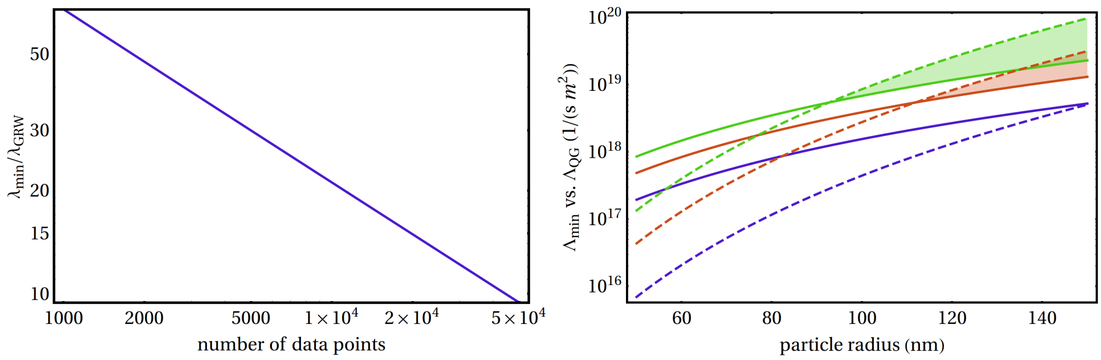

Figure 3.2: On the **(left)** side, we plot the minimum parameter λ over the number of measured data points N, i.e., the minimum parameter λ for the CSL model that we could distinguish from there being no modification to quantum theory. The minimum λ is given in units of the original parameter $\lambda_{\rm GRW} = 10^{-16}$ Hz suggested by Ghirardi, Rimini and Weber [36]. On the **(right)** side, we plot the minimum decoherence parameter $\Lambda_{\rm min}$ discernible by WAX when testing the QG model against the predictions of quantum theory for $N = 50000$ data points. We plot our predictions for three different mass densities of the nanosphere. The solid lines show $\Lambda_{\rm min}$ for $\rho = 2201\,{\rm kg\,m^{-3}}$ (blue), $\rho = 5510\,{\rm kg\,m^{-3}}$ (red), and $\rho = 9680\,{\rm kg\,m^{-3}}$ (green). The dashed lines are the corresponding predictions of $\Lambda_{\rm QG}$ for the QG model, and the shaded regions show where WAX would allow, in principle, to experimentally distinguish between quantum theory and the QG model.

Because macrorealistic models predict decoherence in addition to standard quantum decoherence, macrorealistic models, in general, always predict a larger width for the wavepacket than quantum theory. In order to experimentally determine the occurrence of possible modifications of quantum theory, the experimental error in determining the width of the wavepacket has to be small compared to the expected deviation from quantum theory. We can now ask ourselves, after N experimental runs, what is the minimum additional decoherence $\Lambda_{\rm min}$ we can distinguish from there being no deviation from quantum theory?

In figure 3.2, we show two plots to illustrate this concept for the CSL and the QG model. As we have mentioned earlier, the CSL model depends on two parameters. These parameters are typically denoted as a and λ. a is a length scale that determines the maximum size of superpositions. It is quite consistently chosen to be $a = 100\,\text{nm}$ throughout the literature starting with the original GRW paper [36]. Also in that paper, a value of $\lambda_{\text{GRW}} = 10^{-16}\,\text{Hz}$ was suggested for the second parameter. Various values have been suggested for the latter parameter, ranging from $\lambda_{\text{Adler}} = 4.4 \times 10^{-8\pm2}\,\text{Hz}$ [1] to $\lambda_{\text{CSL}} = 2.2 \times 10^{-17}\,\text{Hz}$. For the plot on the right-hand side of figure 3.2, we keep the parameter $a = 100\,\text{nm}$ constant and calculate the minimum λ we can discern from zero by using the relation

$$\lambda > \lambda_{\text{min}} = \frac{4a^2\Lambda_{\text{min}}}{f(r/a)}\left(\frac{m_0}{m}\right)^2, \tag{3.3}$$

where m_0 is typically the mass of a proton, m is the mass of the nanosphere, r is its radius, and (see Ref. [21]):

$$f(x) = 6x^{-4}\left[1 - 2x^{-2} + (1 + 2x^{-2})\mathrm{e}^{-x^2}\right]. \tag{3.4}$$

From figure 3.2, we conclude that WAX would allow for testing a large parameter range of the CSL model and, for a high enough mass density, would also allow to test the QG model. The DP and the K model, however, cannot be tested using WAX.

3.2 Decoherence in a double-slit experiment (DECIDE)

In DECIDE, a novel version of the double-slit experiment is performed with massive nanospheres. The objective is to determine the features of the interference pattern and to compare the interference visibility with the predictions of quantum theory and to see whether there are any deviations from these predictions due to macrorealistic models.

Figure 3.3 shows the conceptual layout of DECIDE. You may note the similarity to the conceptual layout of WAX in figure 3.1. A typical experimental of DECIDE is very similar to WAX apart from the preparation of the non-classical state and the second time of free evolution:

1. load a nanoparticle into an optical trap inside an optical cavity
2. move the particle to a predefined position along the cavity axis
3. cool the COM motion of the nanoparticle close to the quantum ground state
4. switch off the trap and let the particle's wavefunction expand freely for a time t_1
5. prepare the nanosphere in a quantum superposition similar to a double-slit experiment
6. let the wavefunction expand freely again for a time t_2
7. measure the position of the nanoparticle along the cavity axis
8. trap the particle again and repeat the steps above starting from step (2)

After repeating this procedure often enough to get enough data for statistical significance, the histogram of the measured positions should form an interference pattern. This procedure can be performed for various values of t_1 and t_2 as well as for different particle radii and mass densities in order to determine the parameter dependence of the characteristics of the interference pattern (like fringe spacing and interference visibility). These characteristics can then be determined with the values predicted by quantum theory and with the values predicted by macrorealistic modifications of quantum theory.

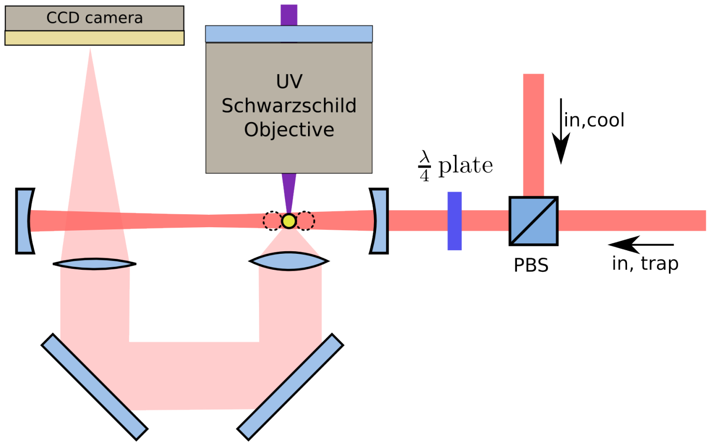

Figure 3.3: **Conceptual design of DECIDE.** The cavity layout is identical to the one in WAX (see figure 3.1). A central additional element is a tightly focused UV beam to prepare the double slit. This is just one possibility of how to prepare the non-classical state of the nanosphere. Other options are discussed in the main text, and in section 5.2. In addition, the dashed circles indicate regions where two IR beams pass vertically out of the plane of the drawing. They originate from a source below the optical bench and are used for detecting when the nanosphere leaves the region we are interested in (see the preliminary design in chapter 4). In that case, light is scattered, collected by the optical system and detected by the CCD camera. The optical path for the imaging of scattered light is indicated via the light red shaded region.

In contrast to WAX, the concept of DECIDE, in principle, allows to test all macrorealistic models we have considered in subsection 2.5.2. Which models we actually want to test, will determine the scientific and resulting technical requirements for performing the experiment.

An essential element of DECIDE is the preparation of the quantum superposition state. At the moment, we see three possibilities how to achieve that:

1. to use a tightly focused beam of short-wavelength light that will locally decohere the wavefunction of the particle and result in a mixed state of a localized state and a quantum superposition state (see also Ref. [47]). The wavelength of the focused laser beam can possibly be chosen longer by using gravity gradients to reduce the time necessary for the two parts of the wavefunction to overlap again after the preparation of the double slit. This novel concept will have to be studied in more detail.
2. to use pulsed light and optomechanical coupling to the position squared for the preparation of the non-classical state (see Refs. [68, 70])
3. to use a tightly focused electron beam from a field-emission electron gun. If the particle is hit, it will be charged and can be discarded via a static electric field. If the particle is not hit, it will be prepared in the desired quantum superposition state. This is a novel concept that will be investigated more closely in the future.

In figure 3.3 and in chapter 4, we will assume the use of the first of these methods, simply because it was the first concept we developed for this purpose and, for that reason, we can describe the necessary technical requirements in detail. The use of the other two methods will require some more study but may result in a significant relaxation of the technical requirements. We will discuss this point in more detail in section 5.2.

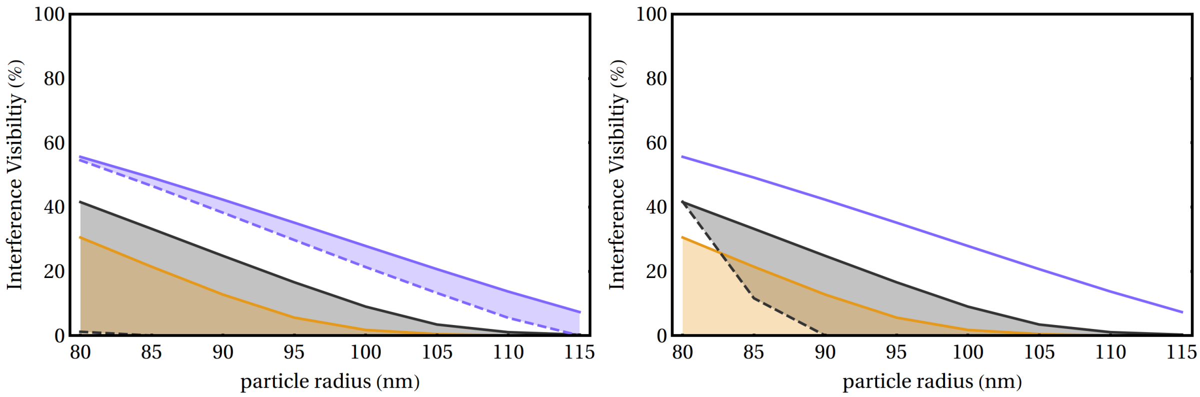

Figure 3.4: **Interference visibilities as functions of the particle radius.** Here, we assumed an environment temperature of 16 K and a particle temperature of 20 K. In the **(left)** plot, we compare the predictions of quantum theory with those of the DP-model, and, in the **(left)** plot, we do the same for the K-model. The solid lines are the predictions of quantum theory for $\rho = 2201\,\mathrm{kg\,m^{-3}}$ (blue), $\rho = 5510\,\mathrm{kg\,m^{-3}}$ (dark gray), and $\rho = 9680\,\mathrm{kg\,m^{-3}}$ (orange). The dashed lines are the corresponding predictions of the Diósi-Penrose model and the model of Károlyházy. The shaded regions show where quantum theory predicts a higher visibility than the respective macrorealistic model. For the K model and a mass density of $\rho = 2201\,\mathrm{kg\,m^{-3}}$, there is no shaded region because the decoherence according to quantum theory is higher than the decoherence predicted by only the K model.

In figure 3.4, we compare the predictions of quantum theory for the interference visibility in DECIDE with the predictions of the DP model (left) and the K model (right). The interference visibilities plotted should **not** be interpreted as exact quantitative predictions because the model used for the predictions is too simple to predict exact values. Despite of that, this model allows us to estimate the parameter dependence (e.g., the dependence on the particle radius), and it allows us to compare the predictions of different theoretical models. Figure 3.4 shows us that, for the experimental parameters assumed in that case, DECIDE would allow for decisive tests of the DP model for all mass densities investigated. For the K model, we need a minimum mass density for a decisive test. It should be noted that here we directly compare the predictions of macrorealistic models and the predictions of quantum theory, i.e., we do not add the decoherence due to macrorealism on top of the standard decoherence due to quantum theory. This simplifies the determination of the experimental parameters allowing for decisive tests of the respective macrorealistic models.

3.3 Baseline-parameters and scientific requirements

Here, we provide an overview of the baseline parameters for WAX and DECIDE. It should be noted, that the scientific requirements for DECIDE are based on the assumption of using a tightly focused short-wavelength beam of light to prepare the quantum superposition. Using a different method, may significantly reduce t_2 and result in **significantly relaxed scientific requirements**. See section 5.2. It should also be noted that the vacuum requirements are **very conservative**. We assumed that there is not a single collision with gas particles during the duration of an experimental run. We are confident that a more detailed analysis will lead to less demanding vacuum requirements. Table 3.1 lists the baseline parameters we assume for WAX and DECIDE.

parameter	value for WAX	value for DECIDE
radius	120 nm	100 nm
nanosphere temperature	60 K	20 K
material absorption at 1064 nm	≤ 0.25 pp**m**/cm	≤ 0.25 pp**b**/cm
environment temperature	32 K	16 K
gas pressure	$< 6 \times 10^{-14}$ Pa	$\lesssim 10^{-14}$ Pa
cavity length	10 cm	10 cm
beam waist	90 μm	90 μm
intra-cavity power	~ 8 W	~ 2.5 W
cavity finesse	≥ 30000	≥ 30000
angular frequency along cavity	113500 rad/s	63000 rad/s
angular frequency perp. to cavity	210 rad/s	116 rad/s
expansion time	100 s	480 s
number of measurements	≤ 50000	≤ 50000
mean occupation number along cavity	≤ 1	0.67
mean occupation number perp. to cavity	$\ll 700$	< 50
readout accuracy	$\ll 60\,\mu$m	$\ll 12\,\mu$m

Table 3.1: **Baseline parameters for WAX and DECIDE.** The parameters for WAX are chosen in order to allow for testing the QG model and a large parameter range of the CSL model. The parameters for DECIDE are chosen to decisively test the QG, the CSL, and the DP model. The vacuum conditions may become significantly relaxed in a less conservative analysis. For DECIDE, several requirements may be relaxed by using alternative methods for preparing the quantum superposition (see section 5.2.

3.4 Technical Requirements

Here, we will provide an overview of the technical requirements for WAX and DECIDE. These requirements, together with an estimation of the respective scientific impact, will be the basis for the trade-off between the experiments, which is discussed in section 3.5. Table 3.2 lists the technical requirements for the two proposed experiments.

3.5 Trade-off and conceptual design selection

In the present study, we performed a trade-off between the proposed experiments in order to determine which of them to study in more detail. Table 3.3 shows that WAX clearly exceeds DECIDE in terms of technical feasibility whereas DECIDE has clear advantages in terms of scientific impact and advantages in terms of the case for space.

WAX is technically less demanding because (1) it does not require the preparation of a quantum superposition, (2) the necessary free-fall times can be shorter than for DECIDE, and the requirements on environment and particle temperature are less demanding. On the other hand, DECIDE excels in terms of scientific impact (see table 3.4) and, for DECIDE, the long free-fall times are not a matter of achieving a higher sensitivity but are necessary in order to see an interference pattern at all.

For the purpose of the present study, we decided to perform a more detailed analysis of DECIDE rather than WAX. The reason is the higher scientific impact of DECIDE as well as the fact that an experimental design capable of performing DECIDE can also be used to perform WAX if one simply does not prepare a quantum superposition but only monitors the expansion of the wavepacket.

requirement on	WAX	DECIDE
	environment	
gas pressure	$\leq 6 \times 10^{-14}$ Pa	$\leq 10^{-14}$ Pa
temperature	32 K	16 K
thermal stability	non-critical	< 0.18 K
	nanosphere	
radius 120 nm	100 nm	
temperature	~ 60 K	20 K
thermal stability	non-critical	< 0.22 K
influence of cosmic rad.	non-critical	non-critical
asymmetry	< 5 %	< 5 %
absorption at 1064 nm	STA	0.25 ppb/cm
mass density	$\geq 2201 \frac{\text{kg}}{\text{m}^3}$	$2201 \frac{\text{kg}}{\text{m}^3}$
	optical setup	
cavity finesse (trap/cool)	~ 30000	~ 30000
position readout accuracy	$\sim 2\,\mu$m	$\sim 2\,\mu$m
pointing stability		
Trap/Cool Cavity mirrors	$< \frac{180\,\mu\text{rad}}{\sqrt{100\,\text{mHz}}}$	$< \frac{180\,\mu\text{rad}}{\sqrt{100\,\text{mHz}}}$
IR beam	$< \frac{180\,\mu\text{rad}}{\sqrt{100\,\text{mHz}}}$	$< \frac{180\mu\text{rad}}{\sqrt{100\,\text{mHz}}}$
UV beam	not applicable	$< 15\mu$rad
thermal stability	$\leq 4.6 \frac{\text{ppm}}{\text{K}}$	$\leq 4.6 \frac{\text{ppm}}{\text{K}}$
IR laser stability	≤ 142 dB RIN at $2\omega_m$	≤ 142 dB RIN at $2\omega_m$
UV laser stability	not applicable	non-critical
UV laser wavelength	not applicable	~ 35 nm
UV laser power	not applicable	$\sim 10^{-15}$ W
	spacecraft	
micro-thruster acc. noise	$\sqrt{\mathcal{S}_A} < 10^{-8}\text{m/s}^2\,\text{Hz}^{-1/2}$	$< 1.6 \times 10^{-9}\text{m/s}^2\,\text{Hz}^{-1/2}$
rotation stability	$\ll 4.5\,\text{mrad}\,\text{Hz}^{-1/2}$	$\ll 240\,\mu\text{rad}\,\text{Hz}^{-1/2}$
quality of micro grav.	$\sqrt{\mathcal{S}_A} < 10^{-8}\text{m/s}^2\,\text{Hz}^{-1/2}$	$< 1.6 \times 10^{-9}\text{m/s}^2\,\text{Hz}^{-1/2}$
change in mass 1 m distance	$\Delta M \leq 39$ kg	$\Delta M \leq 1.6$ kg

Table 3.2: **Technical requirements for WAX and DECIDE.** The values here are chosen for optimal possible performance, i.e., in order for the experiments to test as many macrorealistic theories as possible while not placing too tight technological requirements on the technologies involved. Abbreviations: TBD, to be determined; STA, state of the art.

criterion	WAX	DECIDE
Technical feasibility	+	−
Scientific impact	−	+
Technical complexity	+	−
Risk	+	0
Case for space	0	+

Table 3.3: **Trade-off between the proposed experiments**. We compare the two proposed experiments with respect to several criteria. The symbols + and − denote a relative advantage or disadvantage over the other experiment, respectively. With 0 we denote result that is neither very good nor very bad.

model	WAX	DECIDE
CSL	+	+
QG	+	+
DP	−	+
K	−	0
others	−	0

Table 3.4: **Comparison of the scientific impact of the two experiments**. We compare which macrorealistic models can potentially be tested by WAX and DECIDE. A "+" indicates that the corresponding model can be tested using the respective experiment, while a "−" indicates that this is not possible. Cases where a test may be possible with future improvements are rated as "0". The last row in the table is meant to indicate tests of models beyond those discussed in this study.

4 Preliminary design for DECIDE

DECIDE consists of two subsystems, one outside the spacecraft in order to provide a cryogenic and ultra-high-vacuum environment for the experiment, the other inside the spacecraft. The subsystem outside the spacecraft consists of the **thermal-shield assembly** and the **optical-bench assembly**. The optical-bench assembly is the central part of DECIDE. As much of the experiment as possible is placed inside the spacecraft in order to keep the power dissipation on the external platform to a minimum. In particular, the inner subsystem consists of the **laser assembly**, the **detection assembly** and the **data-preanalysis assembly**. These parts will be described in more detail in the following.

4.1 The thermal-shield assembly

For the thermal shield, we propose to use a design like the one in Ref. [47] as illustrated in figure 4.1, the design of the heat shield proposed for MAQRO [47] is illustrated. The heat shield consists of three shields with decreasing opening angles. We estimated in Ref. [47] that it should be possible to reach a temperature of $30 - 40\,\mathrm{K}$ behind the third shield. The low temperature leads to negligible outgassing (see Ref. [47], allowing vacuum levels below $10^{-12}\,\mathrm{Pa}$. Material outgassed from hot parts of the spacecraft will have too much kinetic energy to be trapped gravitationally in the vicinity of the spacecraft. Studies for optimizing the design of the shield assembly are currently being performed by our partners from EADS Astrium. Using a thermal shield is promising not only for DECIDE also for future missions that would benefit from achieving low temperatures and ultra-high vacuum without the need for active cryogenic cooling and vacuum systems.

4.2 The optical-bench assembly

The optical-bench assembly is the central part of DECIDE. Figure 4.2 shows views of the preliminary design from the top and the bottom. In figure 4.3, the assembly is depicted from the directions indicated in figure 4.2 (left). **Alternatives** to the UV part of this setup are discussed in section 5.2. The preliminary design considered here assumes a very weak ($10^{-15}\,\mathrm{W}$), short-wavelength ($35\,\mathrm{nm}$) UV beam for the preparation of the macroscopic position state. For $35\,\mathrm{nm}$, UV fibers do not exist at the moment but one could conceive using internal reflection along a hollow-core fiber. This is TBD.

The IR fiber is assumed to be polarization maintaining (PM) in order to allow for using a single fiber for the trapping and the cooling/readout field. The same fiber will guide the light reflected from the cavity back to the detection assembly.

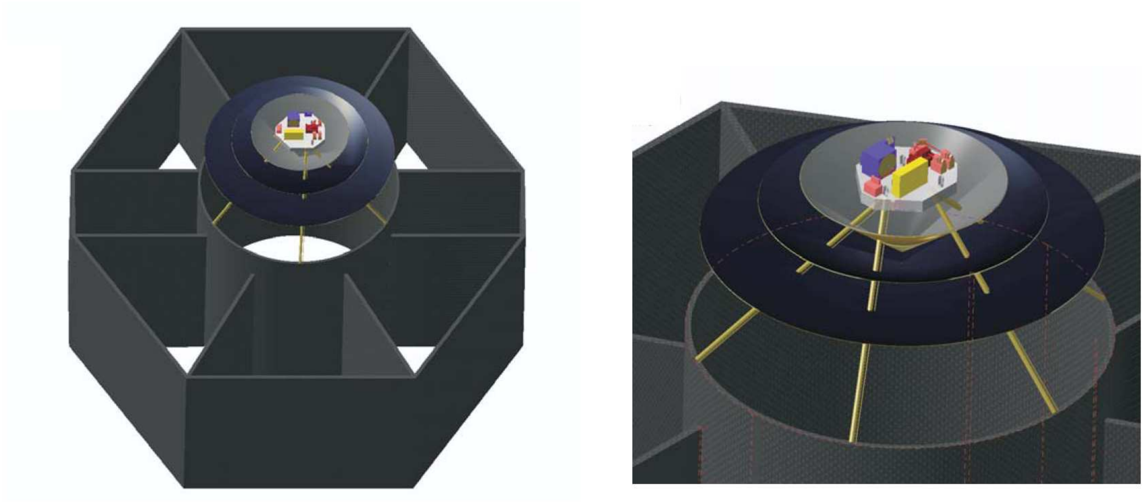

Figure 4.1: **Preliminary design of the heat shield for DECIDE.** The two figures show the heat shield as it was designed in Ref. [47] from two different perspectives. The figures also indicate the position of the optical bench and the struts connecting the heat shield to the structure of the spacecraft.

Optical detection of the position of the nanosphere is achieved by mapping the region of interest (S) onto a CCD/CMOS chip via a combination of lenses (L1 and L2) and mirrors (M2 and M3). The imaging system is kept simple in order to maximize the solid angle for outgassing to space. The cable for the CCD/CMOS chip will depend on the detailed technical implementation of the imaging device. For example, this could be a **spacewire** (see [31]).

The nanospheres are supplied to the cavity by the loading mechanism (LM) below the optical bench (see fig. 4.4). The LM also produces two infrared beams that define a "region of interest" the nanosphere should not leave. A third beam propagates through the middle of the LM structure to propel released nanospheres towards the optical trap.

4.3 The laser assembly and the detection assembly

Figure 4.5 illustrates how the beam from a tunable narrow-band laser is split into two polarization modes for the readout/cooling and the trapping beam. The modes are separated via a polarizing beam splitter (PBS), and each of the modes is modulated by an electro-optic modulator (EOM1 and EOM2) controlled by function generators FG1 and FG2. The modulation of the trapping beam (EOM1) is used for Pound-Drever-Hall (PDH) locking of the laser to the cavity [26, 66]. The cooling/readout beam is a sideband created by EOM2 and shifted by a multiple of the free spectral range (FSR) with respect to the trapping beam. A filtering cavity after EOM2 is used to select the desired sideband. For each mode, a beam splitter (BS) is used to define a local-oscillator mode for homodyne measurements. Then the trapping as well as

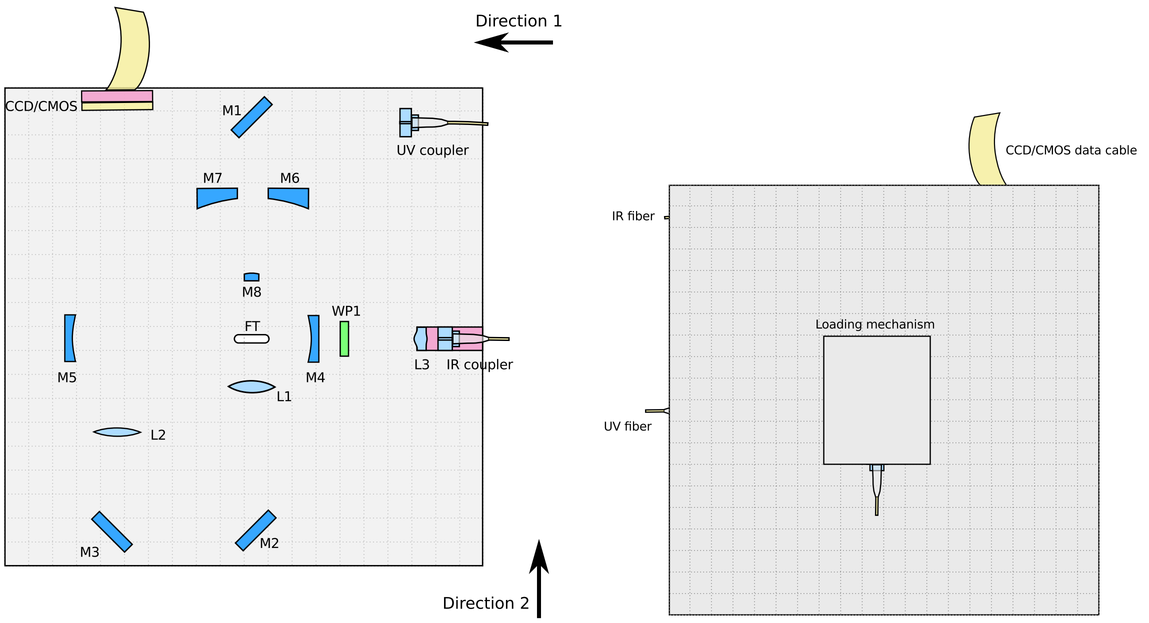

Figure 4.2: The **(left)** and **(right)** figures shows the top and bottom view, respectively, of the preliminary design of the optical bench. The arrows for "Direction 1" and "Direction 2" point out the directions of view for figure 4.3. The dotted lines are separated by intervals of 1 cm. "FT" denotes a a hole in the baseplate for feeding through laser beams and nanospheres from the loading mechanism (LM) located beneath the base plate.

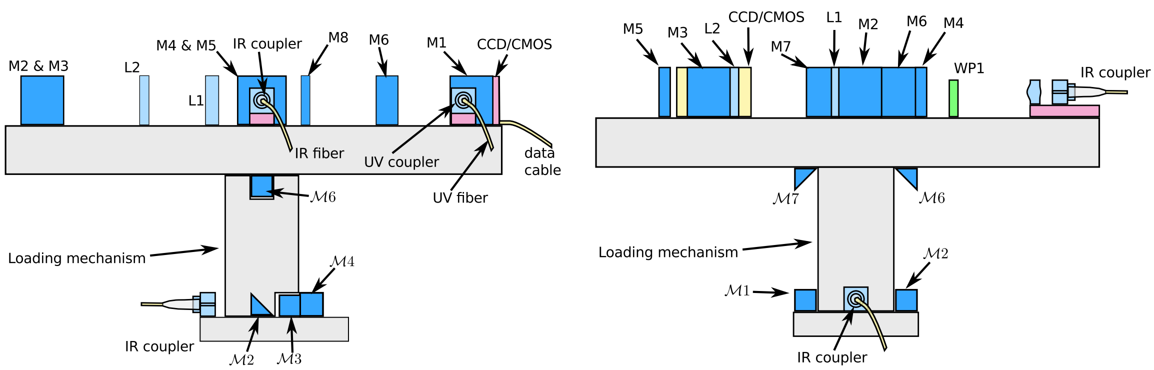

Figure 4.3: The **(left)** and **(right)** figures shows the optical-bench assembly from "Direction 1" and "Direction 2", as described in figure 4.2(left). The size of the base plate is $20 \times 20 \times \text{cm}^2$. On the (right), some of the optical elements are not shown, e.g., the UV coupler.

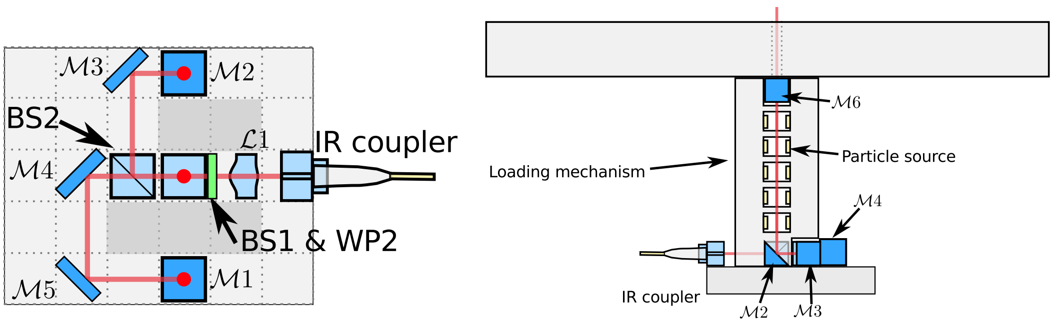

Figure 4.4: The loading-mechanism (LM). **(left)** An IR beam is split into three parts that are reflected out of the drawing (indicated by three red disks) via the prism mirrors $\mathcal{M}1$ and $\mathcal{M}2$ and the beam splitter BS1. The dark gray regions indicate where the bottom plate connects to the rest of the LM structure, which is shown in the (right) figure. The beam inside the LM structure passes several particle sources.

the cooling/readout mode are overlapped at a PBS sent to the optical-bench assembly. Light reflected from the optical bench is separated from the outgoing light via a circulator and is fed to the detection assembly for homodyne detection and for the generation of the PDH error signal. The CCD/CMOS control is not shown.

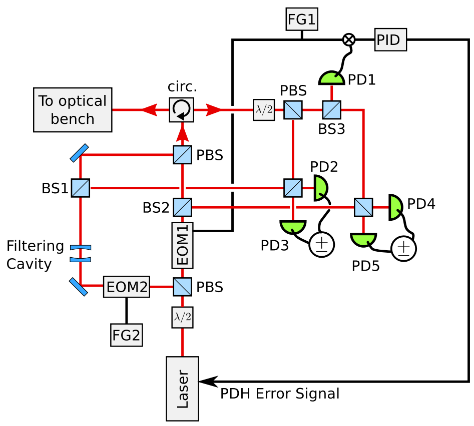

Figure 4.5: **IR laser, modulation, locking and homodyne detection.**

4.4 The data-preanalysis assembly

This assembly comprises the image and spectrum analyzers. They analyze the data and send relevant information to the ground station. On demand, full data sets can be accessed as well.

5 Conclusions

We have presented two experiments, WAX and DECIDE, based on quantum optomechanics with optically trapped nanospheres. Both of them are designed to test quantum theory in a parameter regime where several theories predict modifications of quantum theory to become apparent.

Based on a trade-off between WAX and DECIDE, we chose to investigate DECIDE in further detail for the present study. Given the baseline parameters presented here, DECIDE should allow to test three out of the four macrorealistic modifications of quantum theory discussed in our study. This would extend the parameter regime over which quantum theory has been tested by up to **6 orders of magnitude** – with particles that can, in principle, be seen by the naked eye. The novel concept of DECIDE provides a complementary approach to existing and planned space missions (STE-QUEST, MICROSCOPE, etc.) that test for deviations from the predictions of general relativity due to extensions of the standard model of physics like, e.g., super-symmetry.

For the preliminary design described, DECIDE demands significantly stronger technical requirements but also promises a higher scientific impact than WAX. In section 5.2, we outline possible alternatives to our preliminary design that have the potential to relax those technical requirements, bringing us closer to a realization of DECIDE with technology that is available today or can be expected to be available in the near future.

5.1 Issues that need more detailed analysis or further study

Here, we will review issues that need some further study and consideration.

5.1.1 COM heating due to intracavity power fluctuations

For WAX as well as for DECIDE, the intracavity relative intensity noise has to be to be less than $-142\,\mathrm{dB}$ at twice the mechanical frequency. By using an appropriate mechanism to lock the laser to the cavity and possibly by using an additional filtering cavity or feedback mechanisms as they are uses in the LISA Technology Package, this requirement should be achievable. This will be investigated in more detail.

5.1.2 Cooling the radial degree of freedom

For WAX and DECIDE, it is necessary to cool the occupation number of the radial motion of the nanosphere relatively close to the ground state. This requires sensitive and low-noise feedback mechanisms. This will be investigated in more detail.

5.1.3 Loading nanospheres into the optical trap

The loading mechanism is critical for both experiments. We are currently working on a proof-of-principle realization of such a technique in a study funded by ESA.

5.1.4 Manipulation of the nanospheres

After loading or detection, the nanospheres typically will not be exactly at the position where we need them to be for the next experimental run. That means, we need a mechanism to move the nanospheres along the cavity axis to a predefined position. The best ways for implementing such a mechanism are TBD and to be tested in a lab environment.

Mathematical description of the wavepacket expansion

Our model for predicting the interference fringe spacing and the parameter dependence of the interference visibility needs improvement in order to

- achieve more accurate, quantitative predictions of the interference pattern and its visibility
- get a confirmation of the estimates we have made so far
- investigate the parameter dependence of the interference pattern more closely
- try optimizing the parameters for higher visibility and shorter expansion times

Mathematical description of the double-slit preparation

While we are confident that our description of the density matrix after the application of the UV pulse is a reasonable approximation, a more detailed analysis of the evolution of the density matrix under very well localized and short-wavelength decoherence may lead to more detailed estimates and a possible relaxation of the technical requirements.

5.2 Critical issues and possible solutions

Here, we will provide an overview of critical issues for DECIDE and provide possible solutions and/or alternative approaches in order to overcome these issues.

5.2.1 Preparing the quantum superposition with short-wavelength UV light

As we have mentioned earlier, preparing the quantum superposition this way is only one possibility and alternatives will be discussed in the next subsection 5.2.2. But first, let us discuss the method we have suggested here and possible further investigation and improvements.

The UV light source

UV laser sources with wavelengths as short as 35 nm are far from being off-the-shelf and even further from being applicable in a space environment. **However**, the power we need for preparing the quantum superposition is negligibly small ($\sim 10^{-15}$ W). For such a low power, it may be possible to find a significantly simpler solution with existing sources. This is TBD.

The UV fiber

Fibers for wavelengths $\ll 250\,\mathrm{nm}$ are not available. A possible solution may be to investigate hollow-core fibers that guide short-wavelength UV light via internal reflection. This is TBD.

Charging and damage of the nanosphere for short UV wavelengths

For very short UV wavelengths, silica is not transparent anymore, and the absorption of the photons may result in charging or damaging of the material. This may rule out the use of short UV wavelengths and will have TBD in more detail.

Expansion time

The reason for using 35 nm UV light was that our original assumption of using 350 nm light resulted in free-fall times of several hours per run. By reducing the wavelength, we were able to achieve reasonable times for fused silica but not for materials with a higher mass density. Further reduction of the wavelength is not a solution because of technical reasons and because we would need a new mathematical approach to allow for non-diffraction-limited UV spots.

5.2.2 Possible alternatives to the use of short-wavelength UV light

Here, we will discuss possible alternatives for preparing the quantum superposition in DECIDE. While these alternatives need further investigation, there is significant potential for overcoming the limitations of the UV-based approach.

Preparation of the double slit using pulsed optomechanics

Refs. [68, 70] suggest using pulsed optomechanics in order to prepare a macroscopic quantum superposition. In these proposals, a short pulse, that couples quadratically to the COM position of the nanosphere. A homodyne measurement of the light reflected from the cavity yields a value for the square of the nanosphere position. If the measured value fulfills certain criteria, the nanosphere will be in the desired quantum superposition, otherwise one starts over.

This technique has several advantages over the method using a UV pulse:

- Well defined, narrow “slits”
- Pure superposition states instead of statistical mixtures.
- Arbitrary distance of the two “slits”
- Shorter free-fall times
- Simple analytic description

We are currently considering a modification of the original design to make it suitable for space.

Preparation of the double slit using an electron beam

We mentioned before that short-wavelength UV light could damage or charge the nanosphere. The idea here is to do use that as an advantage, i.e., charge the nanosphere on purpose. The advantage is that we know what is happening to the nanosphere if it is hit, and then we can remove the nanosphere by applying a static electric field. This way, we will end up with a pure quantum superposition state if the sphere is not charged. A possible implementation may use a focused electron beam, e.g., from a field-emission electron gun, for that purpose. Disadvantages may be (1) that we will often have to reload the trap, which requires a fast loading mechanism and nearly identical nanospheres, and (2) that the preparation and focusing of the electron beam may require bulky and power consuming equipment. This is TBD.

Preparation of the double slit with moderate UV wavelengths

We have mentioned that the free-fall times for moderate UV wavelengths (≥ 250 nm) are too long to be practical. Here, we suggest a method to reduce these times. The idea is that during free-fall times on the order of 100 s even tiny gravitational field gradients lead to significant displacements of the nanosphere. We propose to design the optical bench such that there is a small, inhomogeneous gravitational gradient along the cavity axis towards the center of the quantum superposition. This would reduce the free-fall times and may allow using moderate UV wavelengths. This is TBD.

5.3 Technology roadmap

A few aspects of WAX and DECIDE need further study, and some of the technologies will need to be developed and/or demonstrated in proof-of-principle experiments on the way towards a space-based implementation. For this purpose, we outline a technology roadmap indicating the steps towards an eventual space experiment for DECIDE and/or WAX. Some of these steps are currently being worked on already.

1. **Optimization of the thermal-shield design:**
   A detailed thermal study of the design proposed shall be made, and it shall be optimized to achieve as low temperatures as possible. *Currently being done.*
2. **Preparation of macroscopic superpositions (theoretical study):**
   In the current study, we investigated one method to prepare a macroscopic superposition, and we outlined several alternatives methods. This study would investigate all of these methods, compare them and then study the best method in detail. *Currently being done.*
3. **Material study for optically trapped nanoparticles:**
   For experiments on optically trapped particles, it is essential to know the material properties of the particles (absorption, polarizability, etc.).
4. **Laboratory demonstration of cavity and feed-back cooling of optically trapped nanoparticles:**
   A proof-of-principle experiment demonstrating techniques necessary for optomechanical experiments with optically trapped particles. *Currently being done.*
5. **Lab-test of the expansion of the wavefunction and the preparation of a macroscopic superposition:**
   A proof-of-principle experiment for WAX and DECIDE.
6. **Design of a breadboard model for DECIDE:**
   Same functionality as the flight model apart from dimensions, mass, power consumption.

Bibliography

[1] Stephen L Adler. Lower and upper bounds on csl parameters from latent image formation and igm heating. *Journal of Physics A: Mathematical and Theoretical*, 40(12):2935, 2007. 16

[2] O. Arcizet, P.-F. Cohadon, T. Briant, M. Pinard, and A. Heidmann. Radiation-pressure cooling and optomechanical instability of a micromirror. *Nature*, 444:71–74, 2006. 11

[3] O. Arcizet, P.-F. Cohadon, T. Briant, M. Pinard, A. Heidmann, J.-M. Mackowski, C. Michel, L. Pinard, O. Français, and L. Rousseau. High-sensitivity optical monitoring of a micro-mechanical resonator with a quantum-limited optomechanical sensor. *Phys. Rev. Lett.*, 97:133601, 2006. 11

[4] M. Arndt, O. Nairz, J. Voss-Andreae, C. Keller, G. Van der Zouw, and A. Zeilinger. Wave-particle duality of C60 molecules. *Nature*, 401:680–682, 1999. 10

[5] A. Ashkin. Acceleration and Trapping of Particles by Radiation Pressure. *Phys. Rev. Lett.*, 24(4):156–159, Jan 1970. 13

[6] A. Ashkin. Optical trapping and manipulation of neutral particles using lasers. *Proceedings of the National Academy of Sciences*, 94(10):4853–4860, May 1997. 13

[7] M. Aspelmeyer. Quantum mechanics: The surf is up. *Nature*, 464:685–686, April 2010. 11

[8] P. F. Barker and M. N. Shneider. Cavity cooling of an optically trapped nanoparticle. *Phys. Rev. A*, 81:023826, Feb 2010. 13

[9] Adolfo Giuseppe Bartoli. *Sopra i movimenti prodotti dalla luce e dal calore e sopra il radiometro di Crookes*. Le Monnier, Florence, 1876. 10

[10] S. Bose, K. Jacobs, and P. L. Knight. Preparation of nonclassical states in cavities with a moving mirror. *Phys. Rev. A*, 56(5):4175–4186, Nov 1997. 11

[11] V. B. Braginsky and A. B. Manukin. Ponderomotive effects of electromagnetic radiation. *Soviet Physics JETP*, 25:653, 1967. 10

[12] V. B. Braginsky and A. B. Manukin. *Measurement of weak forces in Physics experiments*. Univ. of Chicago Press, 1977. 10

[13] Vladimir B. Braginsky and Yurii I. Vorontsov. Quantum-mechanical limitations in macroscopic experiments and modern experimental technique. *Sov. Phys. Usp.*, 17:644–650, 1975. 10

[14] B. Brezger, L. Hackermüller, S. Uttenthaler, J. Petschinka, M. Arndt, and A. Zeilinger. Matter-Wave Interferometer for Large Molecules. *Phys. Rev. Lett.*, 88:100404, 2002. 10

[15] T. Briant, P.F. Cohadon, M. Pinard, and A. Heidmann. Optical phase-space reconstruction of mirror motion at the attometer level. *Eur. Phys. J. D*, 22:131–140, 2003. 11

[16] Davisson C. and L. H. Germer. The scattering of electrons by a single crystal of nickel. *Nature*, 119:558–560, 1927. 10

[17] Carlton M. Caves. Quantum-Mechanical Radiation-Pressure Fluctuations in an Interferometer. *Phys. Rev. Lett.*, 45(2):75–79, July 1980. 10

[18] Jasper Chan, T. P. Mayer Alegre, Amir H. Safavi-Naeini, Jeff T. Hill, Alex Krause, Simon Gröblacher, Markus Aspelmeyer, and Oskar Painter. Laser cooling of a nanomechanical oscillator into its quantum ground state. *Nature*, 478(7367):89–92, October 2011. 11

[19] D. E. Chang, C. A. Regal, S. B. Papp, D. J. Wilson, J. Y, O. Painter, H. J. Kimble, and P. Zoller. Cavity opto-mechanics using an optically levitated nanosphere. *Proc. Natl. Acad. Sci. USA*, 107:online publication doi:10.1073/pnas.0912969107, 2009. 13

[20] P.-F. Cohadon, A. Heidmann, and M. Pinard. Cooling of a Mirror by Radiation Pressure. *Phys. Rev. Lett.*, 83(16):3174–3177, 10 1999. 11

[21] Brian Collett and Philip Pearle. Wavefunction Collapse and Random Walk. *Foundations of Physics*, 33:1495–1541, 2003. 10.1023/A:1026048530567. 12, 16

[22] Thomas Corbitt, Yanbei Chen, Edith Innerhofer, Helge Müller-Ebhardt, David Ottaway, Henning Rehbein, Daniel Sigg, Stanley Whitcomb, Christopher Wipf, and Nergis Mavalvala. An All-Optical Trap for a Gram-Scale Mirror. *Phys. Rev. Lett.*, 98:150802, 2007. 11

[23] L. Diósi. Gravitation and quantum-mechanical localization of macro-objects. *Physics Letters A*, 105(4–5):199 – 202, 1984. 12

[24] Lajos Diósi. Notes on certain newton gravity mechanisms of wavefunction localization and decoherence. *Journal of Physics A: Mathematical and Theoretical*, 40(12):2989, 2007. 12

[25] A. Dorsel, J. D. McCullen, P. Meystre, E. Vignes, and H. Walther. Optical Bistability and Mirror Confinement Induced by Radiation Pressure. *Phys. Rev. Lett.*, 51:1550–1553, 10 1983. 10, 11

[26] R.W.P. Drever, J.L. Hall, F.V. Kowalski, J. Hough, G.M. Ford, A.J. Munley, and H. Ward. Laser phase and frequency stabilization using an optical resonator. *Applied Physics B*, 31:97–105, 1983. 24

[27] J. Ellis, N. E. Mavromatos, and D. V. Nanopoulos. String theory modifies quantum mechanics. *Physics Letters B*, 293(1–2):37 – 48, 1992. 12

[28] J. Ellis, S. Mohanty, and D. V. Nanopoulos. Quantum gravity and the collapse of the wavefunction. *Physics Letters B*, 221(2):113 – 119, 1989.

[29] John Ellis, John S. Hagelin, D. V. Nanopoulos, and M. Srednicki. Search for violations of quantum mechanics. *Nuclear Physics B*, 241(2):381–405, July 1984. 12

[30] Immanuel Estermann and Otto Stern. Beugung von Molekularstrahlen. *Z. Phys.*, 61:95–125, 1930. 10

[31] European Space Agency. http://www.spacewire.esa.int. 2012. 24

[32] C. Fabre, M. Pinard, S. Bourzeix, A. Heidmann, E. Giacobino, and S. Reynaud. Quantum-noise reduction using a cavity with a movable mirror. *Phys. Rev. A*, 49(2):1337–1343, 1994. 11

[33] R. Feynman, R. B. Leighton, and M. L. Sands. *The Feynman Lectures on Physics, Vol III, Quantum Mechanics*. Addison Wesley, Reading (Mass.), 1965. 9

[34] Andor Frenkel. Spontaneous Localizations of the Wave Function and Classical Behavior. *Found. Phys.*, 20:159, 1990. 12

[35] Stefan Gerlich, Lucia Hackermüller, Klaus Hornberger, Alexander Stibor, Hendrik Ulbricht, Michael Gring, Fabienne Goldfarb, Tim Savas, Marcel Müri, Marcel Mayor, and Markus Arndt. A Kapitza-Dirac-Talbot-lau interferometer for highly polarizable molecules. *Nature Phys.*, 3:711 – 715, 2007. 10

[36] G. C. Ghirardi, A. Rimini, and T. Weber. Unified dynamics for microscopic and macroscopic systems. *Phys. Rev. D*, 34(2):470–491, Jul 1986. 12, 15, 16

[37] Jan Gieseler, Bradley Deutsch, Romain Quidant, and Lukas Novotny. Subkelvin Parametric Feedback Cooling of a Laser-Trapped Nanoparticle. *Phys. Rev. Lett.*, 109:103603, Sep 2012. 13

[38] S. Gigan, H. R. Böhm, M. Paternostro, F. Blaser, G. Langer, J. B. Hertzberg, K. C. Schwab, D. Bäuerle, M. Aspelmeyer, and A. Zeilinger. Self-cooling of a micromirror by radiation pressure. *Nature*, 444:67–70, November 2006. 11

[39] N. Gisin. Stochastic quantum dynamics and relativity. *Helv. Phys. Acta*, 62:363–371, 1989. 12

[40] S. Gröblacher, S. Gigan, H. R. Böhm, A. Zeilinger, and M. Aspelmeyer. Radiation-pressure self-cooling of a micromirror in a cryogenic environment. *Eur. Phys. Lett.*, 81:54003, 2008. 11

[41] Simon Gröblacher, Klemens Hammerer, Michael R. Vanner, and Markus Aspelmeyer. Observation of strong coupling between a micromechanical resonator and an optical cavity field. *Nature*, 460:724–727, August 2009. 11

[42] Simon Gröblacher, Jared B. Hertzberg, Michael R. Vanner, Garrett D. Cole, Sylvain Gigan, K. C. Schwab, and Markus Aspelmeyer. Demonstration of an ultracold micro-optomechanical oscillator in a cryogenic cavity. *Nature Physics*, 5:485–488, June 2009. 11

[43] Lucia Hackermüller, Klaus Hornberger, Björn Brezger, Anton Zeilinger, and Markus Arndt. Decoherence of matter waves by thermal emission of radiatio. *Nature*, 427:711–714, 2004. 10

[44] K. Jacobs, P. Tombesi, M. J. Collett, and D. F. Walls. Quantum-nondemolition measurement of photon number using radiation pressure. *Phys. Rev. A*, 49:1961–1966, 1994. 11

[45] E. Joos and H. D. Zeh. The emergence of classical properties through interaction with the environment. *Zeitschrift fr Physik B Condensed Matter*, 59:223–243, 1985. 10.1007/BF01725541. 12

[46] Thomas Juffmann, Adriana Milic, Michael Müllneritsch, Peter Asenbaum, Alexander Tsukernik, Jens Tüxen, Marcel Mayor, Ori Cheshnovsky, and Markus Arndt. Real-time single-molecule imaging of quantum interference. *Nature Nanotechnology*, 7(5):297–300, May 2012. 10

[47] Rainer Kaltenbaek, Gerald Hechenblaikner, Nikolai Kiesel, Oriol Romero-Isart, Keith C. Schwab, Ulrich Johann, and Markus Aspelmeyer. Macroscopic quantum resonators (MAQRO). *Experimental Astronomy*, 34:123–164, 2012. 12, 13, 17, 23, 24

[48] F. Károlyházy. Gravitation and Quantum Mechanics of Macroscopic Objects. *Nuovo Cimento A*, 52:390, 1966. 12

[49] Johannes Kepler. Letter to Galileo Galilei, April 1610. 10

[50] Johannes Kepler. *De Cometis Libelli Tres.* Augsburg, 1619. 10

[51] T. J. Kippenberg, H. Rokhsari, T. Carmon, A. Scherer, and K. J. Vahala. Analysis of Radiation-Pressure Induced Mechanical Oscillation of an Optical Microcavity. *Phys. Rev. Lett.*, 95:033901, 7 2005. 11

[52] Peter Lebedev. Untersuchungen über die Druckkräfte des Lichtes. *Ann. Phys.*, 6:433–458, 1901. 10

[53] Tongcang Li, Simon Kheifets, and Mark G. Raizen. Millikelvin cooling of an optically trapped microsphere in vacuum. *Nature Physics*, advance on, March 2011. 13

[54] S. Mancini, V. I. Man'ko, and P. Tombesi. Ponderomotive control of quantum macroscopic coherence. *Phys. Rev. A*, 55(4):3042–3050, Apr 1997. 11

[55] S. Mancini and P. Tombesi. Quantum noise reduction by radiation pressure. *Phys. Rev. A*, 49(5):4055–4065, 5 1994. 11

[56] Stefano Mancini, David Vitali, and Paolo Tombesi. Optomechanical Cooling of a Macroscopic Oscillator by Homodyne Feedback. *Phys. Rev. Lett.*, 80:688–691, 1998. 11

[57] William Marshall, Christoph Simon, Roger Penrose, and Dik Bouwmeester. Towards Quantum Superpositions of a Mirror. *Phys. Rev. Lett.*, 91(13):130401, Sep 2003. 11

[58] James Clerk Maxwell. *A treatise on electricity and magnetism*, volume 2. Clarendon Press, Oxford, 1873. 10

[59] P. Meystre, E. M. Wright, J. D. McCullen, and E. Vignes. Theory of radiation-pressure-driven interferometers. *J. Opt. Soc. Am. B*, 2:1830–1840, 1985. 10

[60] Ernest F. Nichols and Gordon F. Hull. About Radiation pressure. *Ann. Phys.*, 12:225–263, 1903. 10

[61] A. D. O'Connell, M. Hofheinz, M. Ansmann, R. C. Bialczak, M. Lenander, E. Lucero, M. Neeley, D. Sank, H. Wang, M. Weides, J. Wenner, J. M. Martinis, and A. N. Cleland. Quantum ground state and single-phonon control of a mechanical resonator. *Nature*, 464:697–703, April 2010. 11

[62] Young-Shin Park and Hailin Wang. Resolved-sideband and cryogenic cooling of an optomechanical resonator. *Nature Phys.*, 5:489–493, 2009. 11

[63] Philip Pearle. Combining stochastic dynamical state-vector reduction with spontaneous localization. *Phys. Rev. A*, 39(5):2277–2289, Mar 1989. 12

[64] R. Penrose. On Gravity's role in Quantum State Reduction. *Gen. Rel. Grav.*, 28:581–600, 1996. 12

[65] M. Pinard, C. Fabre, and A. Heidmann. Quantum-nondemolition measurement of light by a piezoelectric crystal. *Phys. Rev. A*, 51(3):2443–2449, 1995. 11

[66] R. V. Pound. Electronic Frequency Stabilization of Microwave Oscillators. *Review of Scientific Instruments*, 17(11):490–505, 1946. 24

[67] O. Romero-Isart, Mathieu L. Juan, Romain Quidant, and J. Ignacio Cirac. Toward quantum superposition of living organisms. *New J. Phys.*, 12:033015, 2010. 13

[68] O. Romero-Isart, A. C. Pflanzer, F. Blaser, R. Kaltenbaek, N. Kiesel, M. Aspelmeyer, and J. I. Cirac. Large Quantum Superpositions and Interference of Massive Nanometer-Sized Objects. *Phys. Rev. Lett.*, 107(2):020405, Jul 2011. 12, 13, 17, 29

[69] O. Romero-Isart, A. C. Pflanzer, M. L. Juan, R. Quidant, N. Kiesel, M. Aspelmeyer, and J. I. Cirac. Optically levitating dielectrics in the quantum regime: Theory and protocols. *Phys. Rev. A*, 83(1):013803, Jan 2011. 13

[70] Oriol Romero-Isart. Quantum superposition of massive objects and collapse models. *Phys. Rev. A*, 84:052121, Nov 2011. 12, 13, 17, 29

[71] A. Schliesser, O. Arcizet, R. Rivière, G. Anetsberger, and T. J. Kippenberg. Resolved-sideband cooling and position measurement of a micromechanical oscillator close to the heisenberg uncertainty limit. *Nature Physics*, 5:509–514, June 2009. 11

[72] A. Schliesser, P. Del'Haye, N. Nooshi, K. J. Vahala, and T. J. Kippenberg. Radiation Pressure Cooling of a Micromechanical Oscillator Using Dynamical Backaction. *Phys. Rev. Lett.*, 97:243905, 2006. 11

[73] E. Schrödinger. Die gegenwärtige Situation in der Quantenmechanik. *Die Naturwissenschaften*, 23(48):807–812, 1935. 10

[74] J. D. Teufel, T. Donner, Dale Li, J. W. Harlow, M. S. Allman, K. Cicak, A. J. Sirois, J. D. Whittaker, K. W. Lehnert, and R. W. Simmonds. Sideband cooling of micromechanical motion to the quantum ground state. *Nature*, 475(7356):359–363, July 2011. 11

[75] G. P. Thomson. The Diffraction of Cathode Rays by Thin Films of Platinum. *Nature*, 120:802–802, 1927. 10

[76] I. Tittonen, G. Breitenbach, T. Kalkbrenner, T. Müller, R. Conradt, S. Schiller, E. Steinsland, N. Blanc, and N. F. de Rooij. Interferometric measurements of the position of a macroscopic body: Towards observation of quantum limits. *Phys. Rev. A*, 59:1038–1044, 1999. 11

[77] H. von Halban and P. Preiswerk. Experimental evidence of neutron diffraction. *C.R. Hebd. Séances Acad.*, 203:73, 1936. 10

[78] J. Zhang, K. Peng, and S. L. Braunstein. Quantum-state transfer from light to macroscopic oscillators. *Phys. Rev. A*, 68:013808, 2003. 11